Published in final edited form as:
Hepatology. 2014 February ; 59(2): 695–704. doi:10.1002/hep.26683.

Hepatic oxidative stress activates the *Gadd45b* gene via degradation of the transcriptional repressor STAT3

Jung-Hwan Kim[1], **Aijuan Qu**[1], **Janardan K. Reddy**[2], **Bin Gao**[3], and **Frank J. Gonzalez**[1,*]

[1]Laboratory of Metabolism, Center for Cancer Research, National Cancer Institute, National Institutes of Health, Bethesda, Maryland, USA

[2]Department of Pathology, Feinberg School of Medicine, Northwestern University, 303 East Chicago Avenue, Chicago, IL USA

[3]Laboratory of Liver Diseases, National Institute on Alcohol Abuse and Alcoholism, National Institutes of Health, Bethesda, Maryland, USA

Abstract

Growth arrest and DNA damage-inducible beta (GADD45b) plays an important role in many intracellular events, such as cell cycle arrest, DNA repair, cell survival, apoptosis and senescence. However, its mechanism of transcriptional regulation remains unclear. In this study, the mechanism of proliferator-activated receptor α (PPARα) ligand induction of the *Gadd45b* gene in mouse liver was investigated. *Gadd45b* mRNA was markedly induced by the PPARα agonist, Wy-14,643, in wild-type mice but not in *Ppara*-null mice. STAT3 was found to be a repressor of the *Gadd45b* gene through binding to upstream regulatory elements. The role of STAT3 in control of *Gadd45b* was confirmed using liver-specific *Stat3*-null mice. Wy-14,643 treatment stimulated STAT3 ubiquitination leading to activation of the *Gadd45b* gene as a result of loss of *Gadd45b* repression by STAT3. STAT3 degradation was induced by forced overexpression of the PPARα target gene-encoded enzyme ACOX1, that produces increased H_2O_2 as a by product of fatty acid β-oxidation. H_2O_2 also stimulated expression of *Gadd45b* in cultured cells. These studies revealed that PPARα indirectly induces the *Gadd45b* gene in liver through promoting degradation of the repressor STAT3 as a result of elevated oxidative stress.

Keywords

PPARα; GADD45b; STAT3; ACOX1

INTRODUCTION

GADD45b is a sensor molecule that is induced in response to physiological or environmental stressors, and is widely studied for its role in many cellular events, including cell cycle arrest, DNA repair, cell survival and apoptosis, by interplaying with other cellular proteins that are important in cell cycle and stress response machinery, such as PCNA, p21, cdc2/cyclinB and MKK7/JNKK2, a upstream kinase of JNK (1–2). Like above, a posttranslational mechanism of GADD45b regulation was uncovered revealing its function in the cell death/survival pathways by interacting with other molecules. However, the mechanism of transcriptional regulation of the *Gadd45b* gene remains unclear.

*Correspondence: Frank J. Gonzalez, gonzalef@mail.nih.gov; Phone: 301-496-9067; Fax: 301-496-8419.

Peroxisome proliferator-activated receptor α (PPARα), a member of the nuclear receptor superfamily, is a xenobiotic or endogenous ligand-activated transcription factor and plays a critical role in lipid metabolism, inflammation and carcinogenesis in the liver (3–4). PPARα is activated in the liver as a response to starvation where it induces genes involved in fatty acid transport and β-oxidation, and gluconeogenesis (5). Also it is activated by endogenous fatty acid metabolites such as phosphatidylcholine and by synthetic ligands, including the fibrate class of drugs used clinically to treat hyperlipidemia in humans. In response to ligands, PPARα heterodimerizes with retinoid X receptor alpha (RXRα) followed by binding to specific DNA-response elements in target genes known as peroxisome proliferator response elements (PPREs) (6–7). Chronic treatment of rats and mice with synthetic PPARα agonists leads to hepatocarcinogenesis, a phenomenon that does not occur in humans (8–11). During the course of fatty acid oxidation, the peroxisomal and mitochondrial enzymes that are induced by PPARα produce elevated reactive oxygen species (ROS), notably H_2O_2. Induction of GADD45b by PPARα may be a mechanism of cellular defense to protect the hepatocyte from ROS. In the present study, the role of PPARα activation in regulation of the *Gadd45b* was investigated.

METHODS

Materials

Wy-14,643 and anti-FLAG antibody was purchased from Sigma (St Louis, MO, USA). Customized anti-PPARα antibody was obtained from Affinity Bioreagents (Golden, CO, USA). Anti-STAT3 (for ChIP assay and Western blotting), anti-p21 and anti-GFP antibodies were obtained form Santa Cruz Biotechnology (Santa Cruz, California, USA). Anti-STAT3 (for immunohistology) and anti-pSTAT3 antibodies were purchased from Novus Biologicals (Littleton, CO, USA). Anti-pp65, anti-p65, anti-JNK and anti-pJNK antibodies were obtained from Cell Signaling Technology (Beverly, MA, USA). HRP-conjugated anti-HA antibody was purchased from Roche Applied Science (Indianapolis, IN, USA). Anti-GAPDH antibody was purchased from EMD Millipore (Billerica, MA, USA). JetPEI transfection reagent was purchased from VWR International (Radnor, PA, USA).

Animals

Seven- to eight-week-old male WT and *Ppara*-null mice (129/Sv background, five animals per group) or *Acox1*-null mice (C57BL/6 background, three animals per group) or *Stat3*-floxed (*Stat3*$^{F/F}$) or *Stat3*-floxed (12) mice harboring the albumin-Cre recombinase gene (*Stat3*$^{F/F\text{-}AlbCre}$ on a C57BL/6 background) were housed in a pathogen-free animal facility under standard 12 h light/dark cycle with water and chow *ad libitum*. For Wy-14,643 treatment, mice were fed a normal chow diet (control) or a diet with 0.1% w/w Wy-14,643 (Bioserv, Frenchtown, NJ, USA). The *Ikkb*-floxed mice (*Ikkb*$^{F/F}$)(13), obtained from Michael Karin, were bred to the albumin-Cre recombinase gene (14) (C57BL/6 background) to obtain *Ikkb*$^{F/F\text{-}AlbCre}$ mice. All experiments were carried out under the Association for Assessment and Accreditation of Laboratory Animal Care guidelines with approval from the NCI Animal Care and Use Committee.

Cell culture

Hepa1c1c7 cells from ATCC were maintained at 37°C in a humidified atmosphere of 5% CO_2/95% air in DMEM supplemented with 10% heat-inactivated FBS and 50U/ml of penicillin/streptomycin mixture (Invitrogen). Cells were grown to 60–80% confluence and trypsinized with 0.05% trypsin containing 2 mM EDTA.

Plasmids

For mammalian expression, mouse *Ppara* or *Acox1* coding regions were subcloned into the pEGFPc1 vector (Clontech, Mountain Veiw, CA, USA) using XhoI-BamHI or AscI-PacI (extra added restriction sites), respectively. The *Stat3c* cDNA (provided by Arthur Hurwitz, National Cancer Institute), a dominant positive mutant form for STAT3, was subcloned into the CMV-flag and pmCherry vector using XhoI and BamHI restriction sites. A plasmid encoding HA-ubiquitin was kindly provided by Dong Seok Kim (National Cancer Institute, National Institutes of Health). pHyper-cyto vector (Everogen, Moscow, Russia) was used as an intracellular H_2O_2 sensor.

In vivo DNA delivery

Twenty micrograms of pEGFP-*Acox1* or pHyper-cyto vector were dissolved in 2.2 ml of TransIT-QR delivery solution followed by injection through the tail vein in 3 to 5 sec. One day later, the mice were sacrified or fed with Wy-14,643 diet (0.1% w/w) for 24 h. For H_2O_2 measurment, fresh liver pieces (~3 mm^3) were squeezed on the slide glass by force using a cover glass. Images were taken under GFP-filtered fluorescence microscopy under the same conditions.

Quantitative real-time PCR (qPCR)

Total RNA was isolated from the frozen/fresh mouse liver or Hepa1c1c7 cells using Trizol (Invitrogen, Carlsbad, CA). Complementary DNA (cDNA) was synthesized from 1 μg of total RNA using a SuperScript II reverse transcriptase kit (Invitrogen, Carlsbad, CA). qPCR was performed using an Applied Biosystems Prism 7900HT Sequence Detection System (Foster City, CA). All reactions were performed in a 10 μl volume consisting of 25 ng cDNA, 300 nM of each primer and 5 μl of SYBER Green PCR Master Mix (Applied Biosystems) at 95°C for 10 min and 40 cycles of 95°C for 3 s and 60°C for 30 s. Expression levels of mRNA were normalized to *β-actin* as the internal standard. Primers for the qPCR were designed using qPrimerDepot (http://mouseprimerdepot.nci.nih.gov).

Western blotting

Mouse liver or cultured cells were lysed with RIPA lysis buffer (150 mM NaCl, 0.5% Triton X-100, 50 mM Tris–HCl, pH 7.4, 25 mM NaF, 20 mM EGTA, 1 mM DTT, 1 mM Na_3VO_4 and protease inhibitor cocktail) for 30 min on ice, followed by centrifugation at 14,800g for 15 min. Protein concentrations were measured with bicinchoninic acid (BCA) reagent. Protein (30–60 μg) was electrophoresed on a 4–15% gradient tris-HCl gel (Bio-Rad, Hercules, CA) and transferred onto a polyvinylidene difluoride membrane in tris-glycine buffer (pH 8.4) containing 20% methanol. The membrane was blocked with 5% fat-free dry milk in phosphate buffered saline containing 0.1% Tween-20 (PBST) for 1 h. The membranes were probed with primary antibodies and horseradish peroxidase-conjugated secondary antibodies using standard western blotting procedures. Proteins were visualized using the femto signal chemiluminescent substrate (Pierce) under the image analyzer (Alpha Innotech Corp., San Leandro, CA).

Histological and immunohistochemical analysis

For microscopic and macroscopic examination of mouse liver, fresh livers were fixed in 10% buffered formalin and embedded with paraffin. The tissue sections (4 μm) were stained with hematoxylin and eosin (H&E) (Sigma-Aldrich, St. Louis, MO, USA). Anti-STAT3 antibody was use for immunohistochemistry. *In situ* hybridization for the *Gadd45b* mRNA in the liver samples were analyzed in the Histoserv, Inc (Germantown, MD)

Chromatin immunoprecipitation (ChIP) Assay

Mouse livers were fixed with 40 ml of 1% formaldehyde by perfusion at 4 ml/min followed by neutralization with same amount of 1 X glycine solution. The livers were chopped and filtered under 40 micron-size mesh. The filtered liver samples were washed with cold PBS and centrifuged at 900g for 2 min at 4°C. Chopped liver:PBS (1:1) mixtures (150 to 200 μl) were lysed with 500 μl of lysis buffer (150 mM Tris-HCl, pH 8.0; 10 mM EDTA; 1% SDS; 300 μM PMSF; protease inhibitor cocktail) and washed with same buffer briefly. Then the samples were sonicated using the Bioruptor system (Cosmo Bio, Tokyo, Japan) for 15 min (30 sec ON/30 sec OFF mode) in an ice-water bath and centrifuged at 12,000 rpm for 5 min at 4°C. Each sample (50 μl) was mixed with 450 μl ChIP dilution buffer (0.01% SDS, 1% Triton X-100, 2 mM EDTA, 150 mM NaCl, 20 mM Tris-HCl, pH.8.0, and protease inhibitor cocktail). The samples were pre-incubated with protein A/G magnetic bead (Thermo Scientific, Rockford, IL, USA) for 30 min and washed with equal amount of ChIP dilution buffer to minimize the nonspecific binding. Then samples were incubated with 6 μg of normal rabbit IgG or anti-STAT3 overnight at 4°C in a rotary shaker. After sample washing, DNA was eluted and reverse-crosslinked with 150 μl of freshly prepared 2 X elution buffer (1% SDS and 0.1 M NaHCO3) containing 6 μl of 5 M NaCl and proteinase K at 65°C for 2 h followed by DNA purification using the Qiagen PCR purification kit. Quantitative real time PCR and conventional PCR were performed using 1 μl of ChIP DNA samples from the 50 μl of purified samples using the following primers for the putative STAT3 binding regions in the *Gadd45b* promoter region: R1, 5′-AAA GTT CAG GCC AGC CTC TCG-3′ and 5′-AAG TTT CTC TCC TGA TTT CCC GGC-3′; R2, 5′-TCC CTT TCC GGA AGC TGC GTG AG-3′ and 5′-AAT GTC CCT GGC GTG AGA GG-3′; R3, 5′-CGC CTT TAA TCC CAG CAA GCA CTA-3′ and 5′-TGA CTG TCC TGG AAC TCA CTC TGT-3′; R4, 5′-TAT TCC AGG TTG GGC TAT AGC GGT-3′ and 5′-CTG GTG ATG AAT CCA GGA CTT CGT GAT G-3′; R5, 5′-TCC AGA ATC AGT TTG GAT GCC ACC-3′ and 5′-TTT CAT ACT AGG CCA AGC CTA CCC-3′; R6, 5′-TCC TCT GGG TCA AAG CCC AAG TTT-3′ and 5′-TGT CGC CAG AAC AGA GGG AAG AAA-3. The expect PCR sizes were 82 bp, 80 bp, 96 bp, 81 bp, 85 bp and 117 bp, respectively. Conventional PCR was performed using KOD Hot Start DNA polymerase kit (Millipore, Billerica, MA, USA) under the following reaction conditions: initial activation step at 95°C for 2 min, 29 cycles of 95°C for 20 sec, 60°C for 10 sec, 70°C for 20 sec, and a final extension at 70°C for 1 min. DNA binding enrichment were determined using the method as followed; ½^($Ct_{IgG} - Ct_{input}$): ½^($Ct_{STAT3} - Ct_{input}$).

Statistical analysis

Experimental values are expressed as mean ± SD. Statistical analysis was performed by two-tailed Student's t test or Mann Whiney test for unpaired data, with $p < 0.05$ considered statistically significant.

RESULTS

PPARα agonist Wy-14,643 induced *Gadd45b* mRNA in the wild-type mice but not in *Ppara*-null mice

To investigate the role of PPARα in regulation of *Gadd45b* expression, wild-type (WT) and *Ppara*-null mice were treated for 24 h with Wy-14,643. Wy-14,643 induced mRNAs from *Gadd45b* and *Acox1*, a bonafide PPARα target gene, in the WT mice; no induction was noted in *Ppara*-null mice (Fig. 1A). In addition, *Gadd45b* mRNA induction by Wy-14,643 was also confirmed using *in situ* hybridization (Fig. 1B).

PPARα induction of *Gadd45b* mRNA is not due to binding to the *Gadd45b* promoter region

PPARα activation markedly induced *Gadd45b* mRNA in livers from WT mice but not in *Ppara*-null mice. However, no PPRE was observed in the *Gadd45b* promoter region. A series of *Gadd45b* promoter-luciferase constructs were made (Supporting Fig. 1A) and none of these constructs were activated by Wy-14,643 and PPARα with addition of the obligate dimerization partner RXRα (Suppl. Fig. 1B). Interestingly smaller *Gadd45b* 5′-flanking region showed higher luciferase activity than the longer constructs (Supporting Fig. 1C) suggesting the presence of repression elements in the *Gadd45b* promoter. These data suggest that PPARα was not a direct transcription factor controlling *Gadd45* induction.

Wy-14,643-induced STAT3 reduction results in induction of *Gadd45b* mRNA

Gadd45b induction by PPARα could be regulated directly or indirectly. No PPRE's were detected in the upstream and first exon of the *Gadd45b* gene and reporter gene assays using a PPARα expression vector and Wy-14,643 did not show direct activation of the *Gadd45b* promoter. Based on a previously proposed mechanism on *Gadd45b* regulation (15–16), the expression of NF-κB (p65) and JNK were measured in WT mice and *Ppara*-null mice after treatment with Wy-14,643. Western blotting showed that there were no significant changes in the phosphorylation of JNK between the groups of WT and WT+Wy-14,643, however, phosphorylation of JNK was reduced in both *Ppara*-null and *Ppara*-null +Wy-14,643 groups. In addition, phosphorylation of NF-κB (p65) was markedly decreased preferentially in the Wy-14,643-treated WT mice (Supporting Fig. 2) thus suggesting that NF-κB was not involved in induction by Wy-14,643. Signal transducer and activator of transcription 3 (STAT3) protein was also diminished by Wy-14,643 treatment in WT but not in the *Ppara*-null mice. The level of p21, a cell cycle inhibitor, was determined because it is under control of GADD45b (17–18). The results showed that p21 was highly induced by Wy-14,643 in WT but not in the *Ppara*-null mice (Fig. 2A). To further examine the role of STAT3, *Stat3* mRNA levels were measured in livers from the WT and *Ppara*-null mice after Wy-14,643 treatment; *Stat3* mRNA was significantly decreased only in the WT and not in *Ppara*-null mice treated with Wy-14,643 (Fig. 2B). In agreement with the Western blotting data, nuclear STAT3 was significantly decreased only in Wy-14,643-treated WT mice as revealed by immunohistochemistry (Fig. 2C). To assess more directly STAT3 function in the regulation of *Gadd45b*, Hepa1c1c7 cells were treated for 24 h with different concentrations of VI S3I-201, a STAT3 inhibitor, revealing a robust induction of *Gadd45b* mRNA (Fig. 2D), inactivation of STAT3 (Fig. 2E) and inhibition of cell proliferation (Fig. 2F) in a dose-dependent manner. In addition, primary hepatocytes isolated from the WT and *Ppara*-null mice were treated with VI S3I-201 (150 μM) for 24 h, revealing that chemical inhibition of STAT3 induced the *Gadd45b* mRNA in both WT and *Ppara*-null primary hepatocytes (Supporting Fig. 3).

Increased expression of *Gadd45b* in liver-specific Stat3 knockout mice

To support a role for STAT3 in the regulation of *Gadd45b*, liver samples from $Stat3^{F/F}$ and $Stat3^{F/F\text{-}AlbCre}$ mice were subjected to qPCR measurement of *Gadd45b* mRNA. *Gadd45b* mRNA was markedly elevated in livers of untreated $Stat3^{F/F\text{-}AlbCre}$ (Fig. 3A). *Gadd45b* induction by Wy-14,643 treatment was also robust in both $Stat3^{F/F}$ and $Stat3^{F/F\text{-}AlbCre}$ mice (Supporting Fig 4A) thus providing further *in vivo* evidence that STAT3 may, in part, play a role as a repressor in *Gadd45b* gene regulation. However, the $Stat3^{F/F\text{-}AlbCre}$ model is of limited value to explain the entire signaling cascade involved in *Gadd45b* induction, as no significant changes in p65 phosphorylation were noted in between $Stat3^{F/F}$ or $Stat3^{F/F\text{-}AlbCre}$ mice (Fig. 3B).

Although p-p65 was suppressed by Wy-14,643 treatment suggesting suppression of NF-kB, earlier studies in HeLa cells indicated that NF-kB plays a role in regulation of the human

GADD45B promoter (19). To more directly determine a role for NF-kB in regulation of the *Gadd45b* gene, the *Ikk*$^{F/F\text{-}AlbCre}$ mouse model (20) was used to determine whether this factor is involved in *Gadd45b* induction by Wy-14,643 and PPARα in mouse liver. IKKb is an upstream kinase of NF-kB, and absence of this gene suppresses NF-kB. *Ikkb*$^{F/F}$ and *Ikkb*$^{F/F\text{-}AlbCre}$ mice were fed with/without Wy-14,643 (0.1% w/w) diet for 1 day and hepatic *Gadd45b* mRNA was measured. No difference in *Gadd45b* mRNA induction by Wy-14,643 was noted between the *Ikkb*$^{F/F}$ and *Ikkb*$^{F/F\text{-}AlbCre}$ mice (Supporting Fig. 4B). These results indicate that NF-kB might not be a critical inducting factor involved in *Gadd45b* induction by PPARα in mouse liver.

STAT3 binding to the *Gadd45b* promoter was diminished by Wy-14,643

Based on the results implicating STAT3 in regulation of the *Gadd45b* gene, potential STAT3 binding sites on the 5′-flanking region of *Gadd45b* promoter were found using Genomatix software (http://www.genomatix.de). After selection of possible STAT3 binding regions (Fig. 4A), chromatin immunoprecipitation (ChIP) was performed using anti-STAT3 antibody with WT mice fed Wy-14,643 (0.1%, w/w) diet for 1 day. ChIP analysis showed STAT3 binding to several sites in the 5′-flanking region of the *Gadd45b* promoter; STAT3 was significantly decreased in liver nuclear extracts from Wy-14,643-treated mice (Fig. 4B and 4C).

Gadd45b expression was induced by ACOX1 overexpression in the mouse liver

A potential role for oxidative stress in induction of *Gadd45b* was investigated since Wy-14,643 treatment is known to elevate peroxisomal ACOX1 that produces H_2O_2 as a byproduct of fatty acid β-oxidation. Forced expression of ACOX1 by hydrodynamic tail vein injection with pEGFP-Acox1 in the liver of WT mice significantly induced *Gadd45b* mRNA level (Fig. 5A), decreased STAT3 protein levels and inactivated p65 protein (Fig. 5B). Likewise, transient overexpression of ACOX1 also resulted in lower STAT3 protein expression (Fig. 5C). To further verify these results, *Acox1*-null mice were administered Wy-14,643 for three days and mRNAs encoding *Gadd45b* and the PPARα target genes such as *Acsl1*, *Cyp4a10* and *Acadm* were measured. Wy-14,643 treatment had no effect on *Gadd45b* and other PPARα target gene-encoded mRNAs in the *Acox1*-null mice (Fig. 5D). *Stat3* mRNA (Fig. 5D) and STAT3 protein (Fig. 5E) levels were not changed in Wy-14,643-treated *Acox1*-null and *Acox1*-null mice. Hepatic H_2O_2 levels also showed no significant differences between the two groups (Supporting Fig. 5).

H_2O_2 induced *Gadd45b* and promoted STAT3 inactivation

To more directly determine the role of H_2O_2 in *Gadd45b* induction, Hepa1c1c7 cells were treated with different concentrations of H_2O_2 for 2 h resulting in robust induction of *Gadd45b* mRNA (Fig. 6A) and inhibition of phosphorylation of STAT3 (Fig. 6B). There were no significant changes in the NF-κB activation by H_2O_2 in the early time points (Fig. 6B). WT mice were then subjected to hydrodynamic injection with pHyper-cyto (20 μg) plasmid for one day and fed with Wy-14,643 (0.1% w/w) diet for one day to measure intracellular H_2O_2 using the expressed fluorescent sensor protein, HyPer (21). The results revealed that Wy-14,643 treatment increased of H_2O_2 as shown by increased green fluorescence imaging (Fig. 6C). In addition, H_2O_2 levels were directly measured in the livers of *Acox1*-null and *Acox1*-null+Wy-14,643 mice, revealing no significant differences in either cytosolic or mitochondrial H_2O_2 was noted between the two groups (Supporting Fig. 5).

ROS, especially H_2O_2, can trigger hypoxia (22). Thus hypoxia-related experiments were carried out because *Gadd45b* was not induced by Wy-14,643 in cultured primary hepatocytes (Supporting Fig. 6A). Interestingly, *Gadd45b* mRNA levels from both cobalt

chloride (a hypoxia mimic)-induced and 3% oxygen-induced hypoxia conditions were significantly induced (Supporting Fig. 6B and 6C). These results indicate that hypoxia-related factors may be involved in *Gadd45b* induction.

PPARα activation promotes STAT3 ubiquitination

To investigate whether STAT3 degradation was directly the result of Wy-14,643 PPARα activation, the localization of PPARα and STAT3 was examined. Hepa1c1c7 cells were co-transfected with pEGFP-*Ppara* and pmCherry-*Stat3*c constructs for 24 h followed by fluorescence imaging. EGFP-PPARα and STAT3C were co-localized in the nuclear body (Fig. 7A), regarded as the site for ubiquitin-like post-translation modification (23). A binding assay between EGFP-PPARα and STAT3C was carried out by co-immunoprecipitation (co-IP) with nuclear extracts from Hepa1c1c7 cells. STAT3C was bound directly to the EGFP-PPARα protein and the binding was decreased by Wy-14,643 treatment (Fig. 7B). To explore the mechanism of STAT3 degradation, Hepa1c1c7 cells were co-transfected with plasmids expressing EGFP-PPARα and STAT3C-FLAG in the presence or absence of ubiquitin-HA expression for 24 h and then treated with Wy-14,643 for another 24 h. MG132, a proteasome inhibitor, was treated for 2.5 h prior to cell harvest and nuclear extracts subjected to co-IP using anti-FLAG antibody and blotted against HRP conjugated anti-HA antibody. STAT3C underwent ubiquitin degradation in the presence of Wy-14,643 and its degradation was intensified by MG132 (Fig. 7C).

DISCUSSION

In this study, *Gadd45b* mRNA was significantly induced via PPARα activation (Supporting Fig. 7). Induction was coincident with suppression of STAT3 possibly as a result of increased oxidative stress due to the activity of PPARα-induced ACOX1. Gadd45b was implicated in cell cycle arrest and cell death signaling, and thus *Gadd45b* induction may be involved in PPARα-mediated mouse hepatocarcinogenesis. Indeed, PPARα activators were shown to inhibit apoptosis (24). Suppression of apoptosis is expected to potentiate hepatocarcinogenesis of PPARα activators due to lack of elimination of damaged cells. Because cancer originates from a single cell mutation, cell-to-cell microenvironment is also important in the carcinogenesis process. As shown in a previous report (11), both cancer and necrotic inflammation were observed after long-term treatment with Wy-14,643 (0.1% w/w) in mouse liver. This might be due to imbalanced oxygen homeostasis found in the different microenvironments of cells. Thus, marked induction of *Gadd45b* might play a critical role as a defense mechanism against PPARα activation-induced oxidative stress that occurs as a result of increased fatty acid β-oxidation.

PPARα activation markedly induced *Gadd45b* mRNA in livers from WT mice but not in *Ppara*-null mice. However, no PPRE was observed in the *Gadd45b* promoter region, and heterologous *Gadd45b* promoter-luciferase constructs were not activated by Wy-14,643 and PPARα Thus, PPARα was not a direct transcription factor controlling *Gadd45* induction.

Because GADD45b protein is involved in the cell death/proliferation, some signaling molecules involved in the cell death or proliferation were measured in the four groups of mice (WT, WT+Wy-14,643, *Ppara*-null and *Ppara*-null+Wy-14,643). Interestingly, STAT3 protein levels were significantly reduced only in the WT+Wy-14,643 group. STAT3 found to bind to several upstream sites of the *Gadd45b* gene and repress its activity. STAT3 is a transcription factor implicated in oncogenesis, as constitutive activation of STAT3 was found in many cancers (25) The current study revealed that Wy-14,643 increased STAT3 degradation by ubiquitination, and that STAT3 was a repressor of *Gadd45b* gene. Thus, ligand-activated PPARα decreased STAT3 levels resulting in less repression of the *Gadd45b* gene. According to a previous report (26), *Stat3* transcription can be autoregulated

by STAT3 through cooperation with a cAMP-responsive element-binding protein. Thus, Wy-14,643-mediated STAT3 deficiency may influence the self-renewal of Stat3 mRNA.

The mechanism by which PPARα increases STAT3 ubiquitination and degradation likely involved increase cellular ROS as a result of induction of *Acox1* encoding acyl-CoA oxidase, a peroxisomal enzyme that is rate limiting in β-oxidation of long-chain and very long-chain fatty acids. During this process, electrons are donated to molecular oxygen resulting in the production of H_2O_2 as a byproduct (27). Thus, sustained activation of PPARα increases intracellular H_2O_2 levels may result in elevated oxidative stress. *Acox1*-null mice showed no induction of *Gadd45b* as well as other PPARα target genes, such as *Acsl1*, *Cyp4a10*, and *Acadm*, by Wy-14,643. These studies further indicate that Wy-14,643-induced ACOX might have a pivotal role in induction of *Gadd45b* and possibly other PPARα target genes.

H_2O_2 can be easily removed by intracellular catalase or glutathione peroxidase; however, excessive production of H_2O_2 by Wy-14,643 may result in an imbalance between H_2O_2 and catalase induction or its activity in the mouse liver. In a previous report (28), transgenic mice harboring the human catalase gene [$Tg(CAT)^{+/+}$] mice showed high levels of catalase expression and it was markedly induced by Wy-14,643 diet in the liver. Furthermore, hepatocytes from the $Tg(CAT)^{+/+}$ showed significant resistance against cell viability after H_2O_2 challenge. Like other reactive oxygen species, the role of H_2O_2 is controversial but it was shown that high concentrations of H_2O_2 could induce necrotic cell death, whereas low concentrations of H_2O_2 could induce apoptosis (29–30).

Previous reports showed that H_2O_2 could change the epigenetic profile of genes, such as tumor suppressor RUNX3 or E-cadherin promoter in colorectal or hepatocellular carcinoma respectively (31–32). Thus, it's possible that PPARα-mediated oxidative stress could trigger epigenetic changes on the *Gadd45b* gene because *Gadd45b* is also regulated by DNA methylation as revealed in earlier studies (33–34). Furthermore, based on the present data, PPARα may contribute the STAT3 degradation directly and indirectly.

Supplementary Material

Refer to Web version on PubMed Central for supplementary material.

Acknowledgments

Supported by the National Cancer Institute Intramural Research Program. We thank Michael Karin for the *Ikkb*-floxed mice, Sue Goo Rhee for the pHyper-cyto vector and Dong Seok Kim for the HA-ubiquitin plasmid

ABBREVIATION

PPARα	peroxisome proliferator-activated receptor alpha
Gadd45b	growth arrest and DNA-damage-inducible, beta
STAT3	signal transducer and activator of transcription 3
Acox1	acyl-Coenzyme A oxidase 1, palmitoyl
Acsl1	acyl-CoA synthetase long-chain family member 1
Cyp4a10	cytochrome P450 4a10
Acadm	acy-CoA dehydrogenase, medium chain
H&E	hematoxylin and eosin

References

1. Abdollahi A, Lord KA, Hoffman-Liebermann B, Liebermann DA. Sequence and expression of a cDNA encoding MyD118: a novel myeloid differentiation primary response gene induced by multiple cytokines. Oncogene. 1991; 6:165–167. [PubMed: 1899477]
2. Liebermann DA, Hoffman B. Gadd45 in stress signaling. J Mol Signal. 2008; 3:15. [PubMed: 18789159]
3. Pyper SR, Viswakarma N, Yu S, Reddy JK. PPARα: energy combustion, hypolipidemia, inflammation and cancer. Nucl Recept Signal. 2010; 8:e002. [PubMed: 20414453]
4. Peters JM, Shah YM, Gonzalez FJ. The role of peroxisome proliferator-activated receptors in carcinogenesis and chemoprevention. Nat Rev Cancer. 2012; 12:181–195. [PubMed: 22318237]
5. Kersten S, Seydoux J, Peters JM, Gonzalez FJ, Desvergne B, Wahli W. Peroxisome proliferator-activated receptor α mediates the adaptive response to fasting. J Clin Invest. 1999; 103:1489–1498. [PubMed: 10359558]
6. Chakravarthy MV, Lodhi IJ, Yin L, Malapaka RR, Xu HE, Turk J, Semenkovich CF. Identification of a physiologically relevant endogenous ligand for PPARα in liver. Cell. 2009; 138:476–488. [PubMed: 19646743]
7. Desvergne B, Wahli W. Peroxisome proliferator-activated receptors: nuclear control of metabolism. Endocr Rev. 1999; 20:649–688. [PubMed: 10529898]
8. Hays T, Rusyn I, Burns AM, Kennett MJ, Ward JM, Gonzalez FJ, Peters JM. Role of peroxisome proliferator-activated receptor-α (PPARα) in bezafibrate-induced hepatocarcinogenesis and cholestasis. Carcinogenesis. 2005; 26:219–227. [PubMed: 15447978]
9. Peters JM, Cattley RC, Gonzalez FJ. Role of PPAR α in the mechanism of action of the nongenotoxic carcinogen and peroxisome proliferator Wy-14,643. Carcinogenesis. 1997; 18:2029–2033. [PubMed: 9395198]
10. Klaunig JE, Babich MA, Baetcke KP, Cook JC, Corton JC, David RM, DeLuca JG, et al. PPARα agonist-induced rodent tumors: modes of action and human relevance. Crit Rev Toxicol. 2003; 33:655–780. [PubMed: 14727734]
11. Woods CG, Burns AM, Bradford BU, Ross PK, Kosyk O, Swenberg JA, Cunningham ML, et al. WY-14,643 induced cell proliferation and oxidative stress in mouse liver are independent of NADPH oxidase. Toxicol Sci. 2007; 98:366–374. [PubMed: 17483499]
12. Moh A, Iwamoto Y, Chai GX, Zhang SS, Kano A, Yang DD, Zhang W, et al. Role of STAT3 in liver regeneration: survival, DNA synthesis, inflammatory reaction and liver mass recovery. Lab Invest. 2007; 87:1018–1028. [PubMed: 17660847]
13. Maeda S, Chang L, Li ZW, Luo JL, Leffert H, Karin M. IKKbeta is required for prevention of apoptosis mediated by cell-bound but not by circulating TNFα. Immunity. 2003; 19:725–737. [PubMed: 14614859]
14. Yakar S, Liu JL, Stannard B, Butler A, Accili D, Sauer B, LeRoith D. Normal growth and development in the absence of hepatic insulin-like growth factor I. Proc Natl Acad Sci U S A. 1999; 96:7324–7329. [PubMed: 10377413]
15. De Smaele E, Zazzeroni F, Papa S, Nguyen DU, Jin R, Jones J, Cong R, et al. Induction of gadd45beta by NF-kappaB downregulates pro-apoptotic JNK signalling. Nature. 2001; 414:308–313. [PubMed: 11713530]
16. Papa S, Zazzeroni F, Bubici C, Jayawardena S, Alvarez K, Matsuda S, Nguyen DU, et al. Gadd45 beta mediates the NF-kappa B suppression of JNK signalling by targeting MKK7/JNKK2. Nat Cell Biol. 2004; 6:146–153. [PubMed: 14743220]
17. Vairapandi M, Balliet AG, Fornace AJ Jr, Hoffman B, Liebermann DA. The differentiation primary response gene MyD118, related to GADD45, encodes for a nuclear protein which interacts with PCNA and p21WAF1/CIP1. Oncogene. 1996; 12:2579–2594. [PubMed: 8700517]
18. Shimada H, Sakakima H, Tsuchimochi K, Matsuda F, Komiya S, Goldring MB, Ijiri K. Senescence of chondrocytes in aging articular cartilage: GADD45beta mediates p21 expression in association with C/EBPbeta in senescence-accelerated mice. Pathol Res Pract. 2011; 207:225–231. [PubMed: 21353395]

19. Jin R, De Smaele E, Zazzeroni F, Nguyen DU, Papa S, Jones J, Cox C, et al. Regulation of the gadd45beta promoter by NF-kappaB. DNA Cell Biol. 2002; 21:491–503. [PubMed: 12162804]
20. Maeda S, Kamata H, Luo JL, Leffert H, Karin M. IKKbeta couples hepatocyte death to cytokine-driven compensatory proliferation that promotes chemical hepatocarcinogenesis. Cell. 2005; 121:977–990. [PubMed: 15989949]
21. Rhee SG, Chang TS, Jeong W, Kang D. Methods for detection and measurement of hydrogen peroxide inside and outside of cells. Mol Cells. 2010; 29:539–549. [PubMed: 20526816]
22. Chandel NS, Maltepe E, Goldwasser E, Mathieu CE, Simon MC, Schumacker PT. Mitochondrial reactive oxygen species trigger hypoxia-induced transcription. Proc Natl Acad Sci U S A. 1998; 95:11715–11720. [PubMed: 9751731]
23. Muller S, Matunis MJ, Dejean A. Conjugation with the ubiquitin-related modifier SUMO-1 regulates the partitioning of PML within the nucleus. EMBO J. 1998; 17:61–70. [PubMed: 9427741]
24. Roberts RA, Michel C, Coyle B, Freathy C, Cain K, Boitier E. Regulation of apoptosis by peroxisome proliferators. Toxicol Lett. 2004; 149:37–41. [PubMed: 15093246]
25. Klampfer L. Signal transducers and activators of transcription (STATs): Novel targets of chemopreventive and chemotherapeutic drugs. Curr Cancer Drug Targets. 2006; 6:107–121. [PubMed: 16529541]
26. Ichiba M, Nakajima K, Yamanaka Y, Kiuchi N, Hirano T. Autoregulation of the Stat3 gene through cooperation with a cAMP-responsive element-binding protein. J Biol Chem. 1998; 273:6132–6138. [PubMed: 9497331]
27. Varanasi U, Chu R, Chu S, Espinosa R, LeBeau MM, Reddy JK. Isolation of the human peroxisomal acyl-CoA oxidase gene: organization, promoter analysis, and chromosomal localization. Proc Natl Acad Sci U S A. 1994; 91:3107–3111. [PubMed: 8159712]
28. Chen X, Liang H, Van Remmen H, Vijg J, Richardson A. Catalase transgenic mice: characterization and sensitivity to oxidative stress. Arch Biochem Biophys. 2004; 422:197–210. [PubMed: 14759608]
29. Tochigi M, Inoue T, Suzuki-Karasaki M, Ochiai T, Ra C, Suzuki-Karasaki Y. Hydrogen peroxide induces cell death in human TRAIL-resistant melanoma through intracellular superoxide generation. Int J Oncol. 2013; 42:863–872. [PubMed: 23314732]
30. Troyano A, Sancho P, Fernandez C, de Blas E, Bernardi P, Aller P. The selection between apoptosis and necrosis is differentially regulated in hydrogen peroxide-treated and glutathione-depleted human promonocytic cells. Cell Death Differ. 2003; 10:889–898. [PubMed: 12867996]
31. Kang KA, Zhang R, Kim GY, Bae SC, Hyun JW. Epigenetic changes induced by oxidative stress in colorectal cancer cells: methylation of tumor suppressor RUNX3. Tumour Biol. 2012; 33:403–412. [PubMed: 22274925]
32. Lim SO, Gu JM, Kim MS, Kim HS, Park YN, Park CK, Cho JW, et al. Epigenetic changes induced by reactive oxygen species in hepatocellular carcinoma: methylation of the E-cadherin promoter. Gastroenterology. 2008; 135:2128–2140. 2140 e2121–2128. [PubMed: 18801366]
33. Jiang C, Zhou B, Fan K, Heung E, Xue L, Liu X, Kirschbaum M, et al. A sequential treatment of depsipeptide followed by 5-azacytidine enhances Gadd45beta expression in hepatocellular carcinoma cells. Anticancer Res. 2007; 27:3783–3789. [PubMed: 18225533]
34. Na YK, Lee SM, Hong HS, Kim JB, Park JY, Kim DS. Hypermethylation of growth arrest DNA-damage-inducible gene 45 in non-small cell lung cancer and its relationship with clinicopathologic features. Mol Cells. 2010; 30:89–92. [PubMed: 20652500]

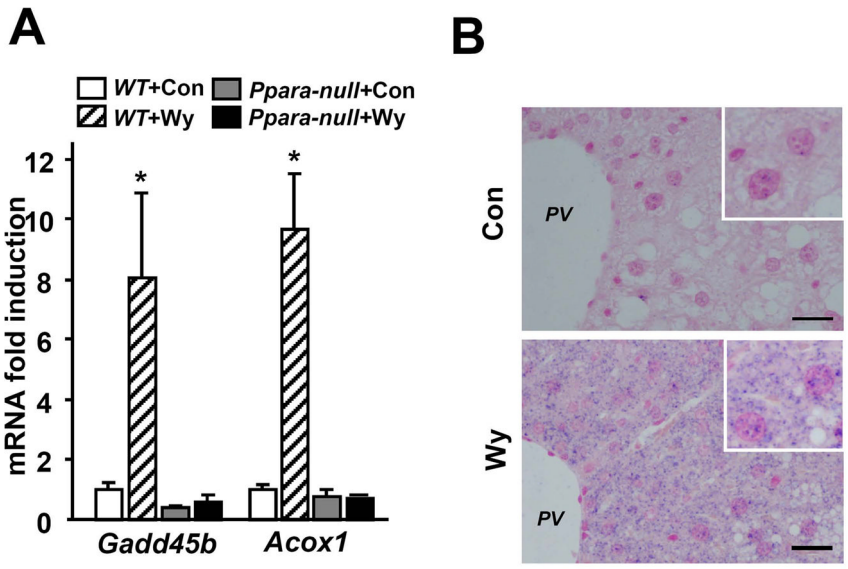

Figure 1. Wy-14,643 induces *Gadd45b* mRNA in the wild-type mice but not in *Ppara*-null mice

A, *Ppara* WT or *Ppara*-null mice were fed with Wy-14,643 (0.1%, w/w) for 1 day. Liver samples were subjected to qPCR. Con, control; WT, wild type; Wy, Wy-14,643. *p<0.0001 (vs WT+Con)

B. *In situ* hybridization for *Gadd45b* mRNA after 1 day treatment with Wy-14,643 (0.1%, w/w) in WT mice. Con, control; Wy, Wy-14,643; PV, portal vein; Purple color, nucleus; Blue color, *Gadd45b* mRNA; Scale bar size, 25 μm

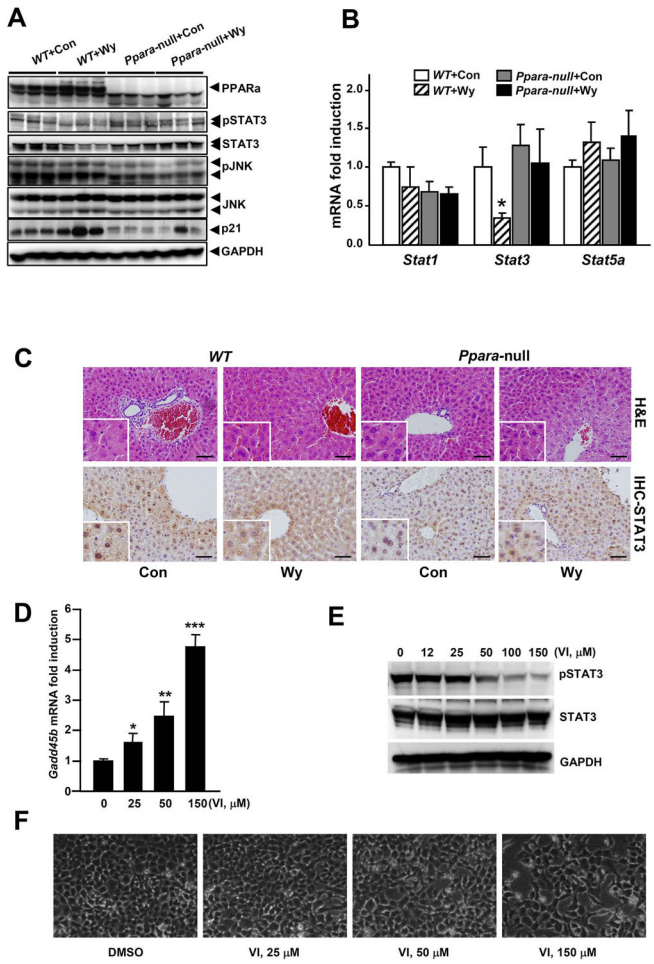

Figure 2. Wy-14,643- induced STAT3 degradation resulted in induction of *Gadd45b* mRNA

A. Western blotting data showed in the liver from WT or *Ppara*-null mice fed with Wy-14,643 (0.1% w/w) for 1day. Con, control; WT, wild-type; Wy, Wy-14,643.

B. qPCR data are shown using samples from (A). Con, control; WT, wild-type; Wy, Wy-14,643. *p<0.05 (vs WT+Con)

C. H&E and Immunohistochemistry were using the liver tissue from WT or *Ppara*-null mice fed Wy-14,643 (0.1% w/w) for 1 day. Con, control; WT, wild type; Wy, Wy-14,643. Scale bar size, 50 μm

D. *Gadd45b* mRNA was measured in Hepa1c1c7 cells treated with different concentration of STAT3 inhibitor (VI, VI S3I-201) for 24 h. *p<0.05, **p<0.001, ***p<0.0001 (vs 0 μM)

E. Hepa1c1c7 cells were treated with different concentration of STAT3 inhibitor for 24 h and cell lysates were subjected to western blot analysis. VI, VI S3I-201.

F. Phase contrast cell images were taken in Hepa1c1c7 cells after STAT3 inhibitor treatments. VI, VI S3I-20; Magnitude, ×5

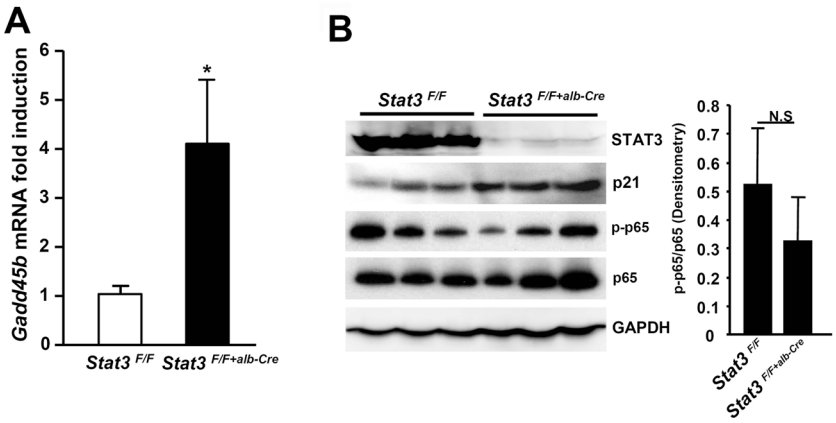

Figure 3. Liver-specific *Stat3* ablation results in increased *Gadd45b* expression

A. *Gadd45b* mRNA expressions were measured in livers from the $Stat3^{F/F}$ or $Stat3^{F/F+alb\text{-}Cre}$ mice treated with/without Wy-14,643. Wy, Wy-14,643; *p<0.05; **p<0.001; N.S, not significant.

B. Protein levels were measured by western blotting in livers from $Stat3^{F/F}$ or $Stat3^{F/F+alb\text{-}Cre}$ mice.

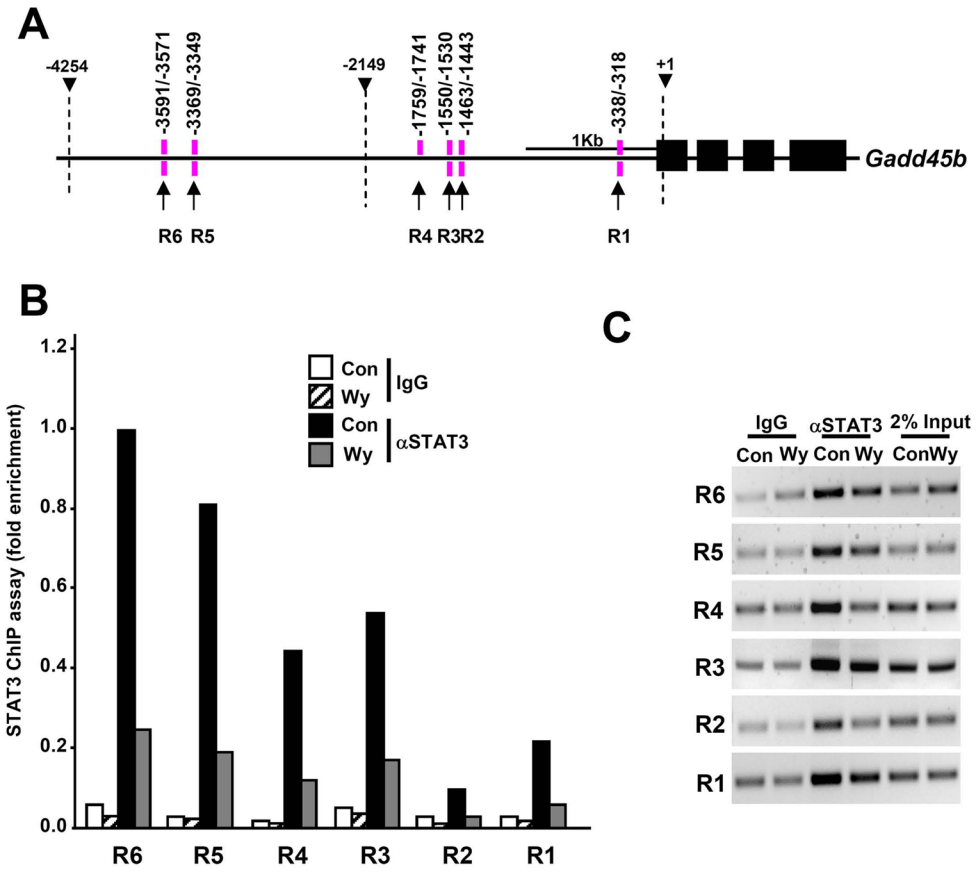

Figure 4. STAT3 binding to the *Gadd45b* promoter region was suppressed by Wy-14,643-induced PPARα activation

A. Putative STAT3 binding sites in *Gadd45b* promoter are shown. Purple-colored bar, predicted STAT3 binding site; R, region.

B. ChIP assay against STAT3 was examined using liver samples from the WT or *Ppara*-null mice fed with Wy-14,643 (0.1% w/w) for 1 day. The ChIP samples were analyzed using the specifically designed primers from R1 to R6.

C. The ChIP samples from (B) were amplified using the conventional PCR method and the amplicons were resolved in 3% agarose gel.

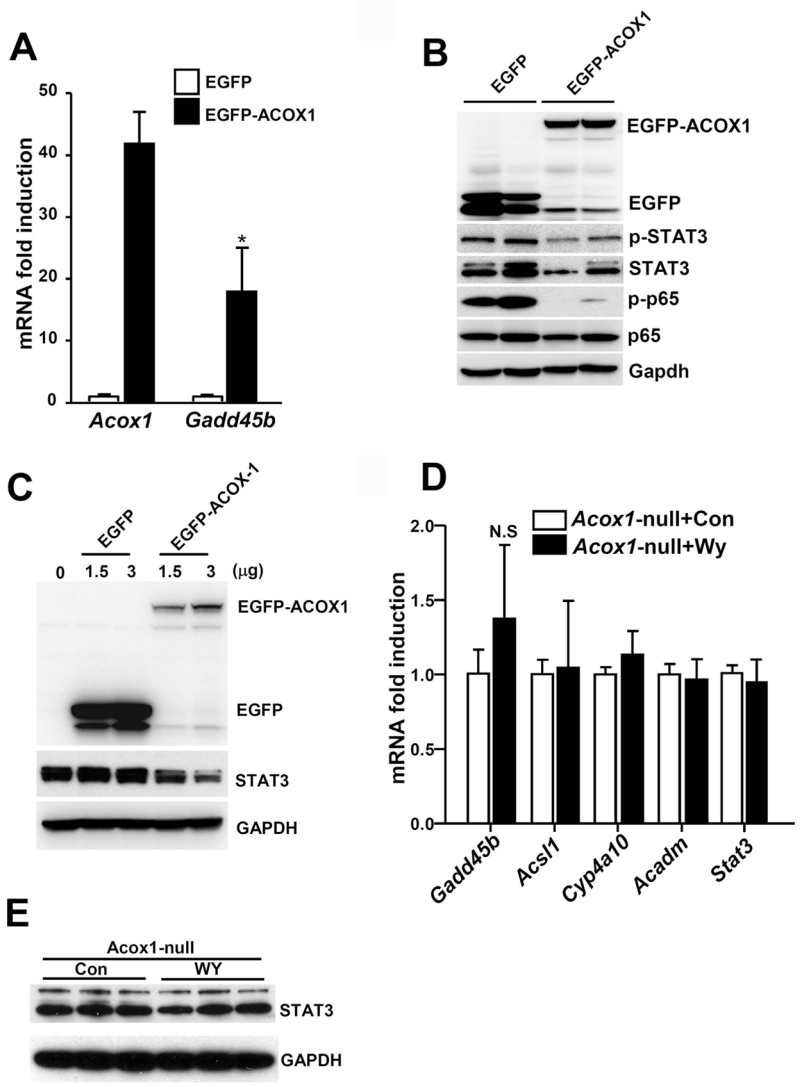

Figure 5. Overexpression of ACOX1 triggeres induction of *Gadd45b* mRNA and STAT3 degradation

A. Hydrodynamic injection of pEGFP-Acox1 construct (20 μg/mouse) was executed and *Acox1* and *Gadd45b* mRNA levels were measured using qPCR method. *p<0.001 (vs EGFP)

B. The same samples from (A) were subjected to Western blotting.

C. Hepa1c1c7 cells were transfected with different amounts of pEGFP or pEGFP-Acox1 plasmids for 24 h and whole cell extracts were subjected to Western blotting.

D. *Gadd45b* and PPARα target mRNAs were measured using the liver samples from the *Acox*-null mice fed Wy-14,643 (0.1% w/w) for three days. N.S, no significant

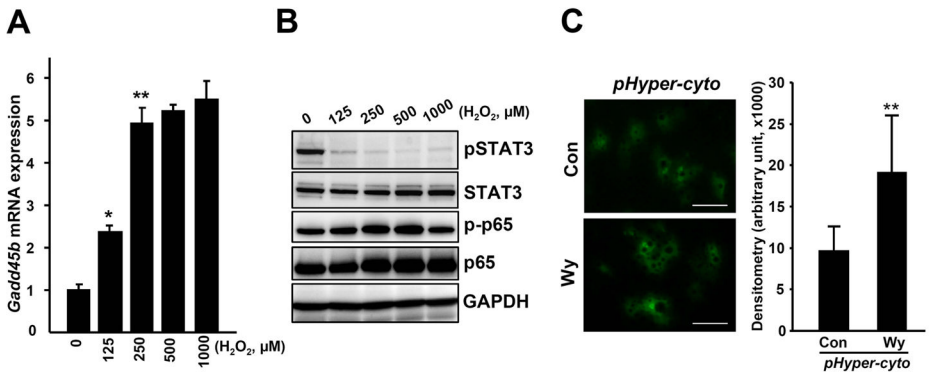

Figure 6.

H_2O_2 induced *Gadd45b* induction and STAT3 inactivation

A. *Gadd45b* mRNA was measured using samples from the Hepa1c1c7 cells treated with different concentration of H_2O_2 for 2 h. *p<0.001; **p<0.0001 (vs 0 M)

B. Western blotting data were subjected using the Hepa1c1c7 cells treated with different concentration of H_2O_2 for 2 h.

C. pHyper-cyto vector, as a H_2O_2 sensor, was injected via tail vein of WT mice using hydrodynamic injection method and fed with Wy-14,643 (0.1% w/w) for 1day. Small liver pieces (~3 mm^3) were squeezed on the slide glass by force using a cover glass. Images were taken under GFP-filtered fluorescence microscopy with same condition. The densitometry of GFP intensity shows in the right. Scale bar size, 50 μm. **p<0.0001 (vs Con)

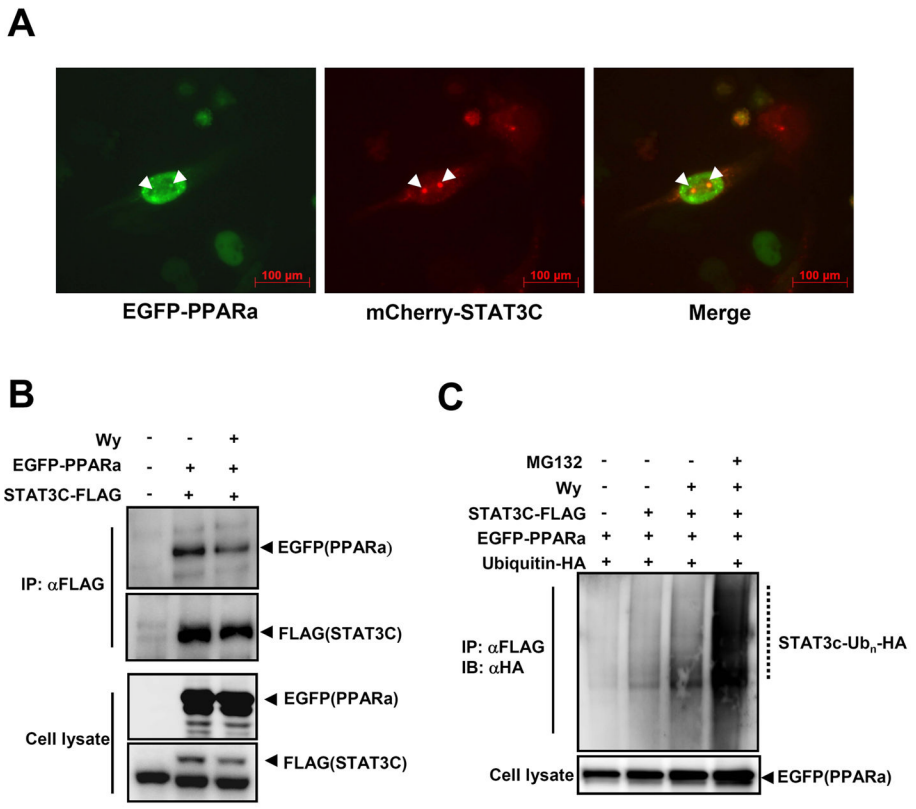

Figure 7. PPARα activation controls STAT3 degradation by ubiquitination

A. Hepa1c1c7 cells were co-transfected with pEGFP-*Ppara* and pmCherry-*Stat3c* for 24 h and images were taken under the fluorescence microscopy.

B. Hepa1c1c7 cells were co-transfected with pEGFP-Ppara and pStat3c-flag for 24 h and treated with Wy-14,643 (10 μM) for 24 h. Nucleus extracts were subjected to immunoprecipitation using anti-FLAG antibody and blotted against anti-GFP. Exogenous protein expressions were measured from the whole cell extract for the control.

C. Hepa1c1c7 cells were co-transfected with pEGFP-Ppara, pStat3c-flag, and pUbiquitin-HA for 24 h and treated with Wy-14,643 (10 μM) for 24 h. The cells then treated with MG132, a proteasome inhibitor, for 2.5 h before cell harvest. Nuclear extracts were subjected to immunoprecipitation with anti-FLAG antibody and blotted against HA antibody. EGFP-PPARa from total lysates was used as a control.